J Mol Model (2013) 19:3369–3383
DOI 10.1007/s00894-013-1861-5

ORIGINAL PAPER

Sequence and structural investigation of a novel psychrophilic α-amylase from *Glaciozyma antarctica* PI12 for cold-adaptation analysis

Aizi Nor Mazila Ramli · Mohd Akmal Azhar · Mohd Shahir Shamsir · Amir Rabu · Abdul Munir Abdul Murad · Nor Muhammad Mahadi · Rosli Md. Illias

Received: 5 February 2013 / Accepted: 18 April 2013 / Published online: 18 May 2013

Abstract A novel α-amylase was isolated successfully from *Glaciozyma antarctica* PI12 using DNA walking and reverse transcription-polymerase chain reaction (RT-PCR) methods. The structure of this psychrophilic α-amylase (AmyPI12) from *G. antarctica* PI12 has yet to be studied in detail. A 3D model of AmyPI12 was built using a homology modelling approach to search for a suitable template and to generate an optimum target–template alignment, followed by model building using MODELLER9.9. Analysis of the AmyPI12 model revealed the presence of binding sites for a conserved calcium ion (CaI), non-conserved calcium ions (CaII and CaIII) and a sodium ion (Na). Compared with its template—the thermostable α-amylase from *Bacillus stearothermophilus* (BSTA)—the binding of CaII, CaIII and Na ions in AmyPI12 was observed to be looser, which suggests that the low stability of AmyPI12 allows the protein to work at different temperature scales. The AmyPI12 amino acid sequence and model were compared with thermophilic α-amylases from *Bacillus* species that provided the highest structural similarities with AmyPI12. These comparative studies will enable identification of possible determinants of cold adaptation.

Keywords Cold-adapted α-amylase · *Glaciozyma antarctica* PI12 · Cold-adaptation · Flexibility

A. N. M. Ramli · M. A. Azhar · R. Md. Illias (✉)
Department of Bioprocess Engineering, Faculty of Chemical Engineering, Universiti Teknologi Malaysia, 81310, Skudai, Johor, Malaysia
e-mail: r-rosli@utm.my

M. S. Shamsir
Faculty of Bioscience and Medical Engineering, Universiti Teknologi Malaysia, 81310, Skudai, Johor, Malaysia

A. Rabu · A. M. A. Murad
School of Biosciences and Biotechnology, Faculty of Science and Technology, Universiti Kebangsaan Malaysia, 43600, Bangi, Selangor, Malaysia

N. M. Mahadi
Malaysia Genome Institute (MGI), Jalan Bangi Lama, 43600, Bangi, Selangor, Malaysia

Introduction

The Earth's biosphere presents a wide spectrum of different environments in which colonization by life requires a large variety of adaptive strategies. Low temperatures are the most widespread extreme condition for life. Organisms adapted to such extreme environments are known as psychrophiles. Currently, the enzymes produced by organisms living in habitats that are characterized by extreme physicochemical conditions are of great interest due to the high adaptive pressure to which they were subjected [1]. Cold-adapted enzymes or cold-active enzymes synthesized by psychrophiles display improved catalytic efficiency at low temperatures that compensate for the inherent reduction in chemical reaction rates. This efficiency is reflected in their higher turnover number and/or increased affinity for substrates compared with their mesophilic and thermophilic counterparts [2]. Optimization of their catalytic parameters can originate from the highly flexible structure of cold-adapted enzymes in either a selected area or in overall protein structure, which provides an enhanced ability to undergo conformational changes during catalysis at low temperatures. This enhanced plasticity appears, in turn, to

be responsible for the thermolability of cold-adapted enzymes, in contrast with the thermostability of enzymes from thermophiles, which is correlated with the rigidity of their polypeptide chain [3]. These particular properties make cold-adapted enzymes potentially unrivalled for numerous biotechnological tasks, particularly for use in industrial processes as energy savers. Furthermore, in this century, due to the energy crisis and the rise of global warming in recent decades, the development of energy-saving products to reduce environmental burdens has become a trend [4].

Various cold-adapted enzymes, including α-amylases, have great potential in various industrial and biotechnological processes. α-Amylases (α-1,4-glucan-4-glucanohydrolases, EC 3.2.1.1) catalyze the hydrolysis of α-(1,4) glycosidic linkages of glycogen, starch, related polysaccharides and some oligosaccharides. α-Amylases are widely distributed in various bacteria, fungi, plants and animals, and play major roles in the utilization of polysaccharides [5]. In addition, the α-amylase family comprises the largest family of glycoside hydrolases, with the majority of enzymes acting on starch, glycogen and related oligo- and polysaccharides. The protein forms of these enzymes typically comprise three domains: A, B and C. Domain A is a $(\beta/\alpha)_8$-barrel, domain B is a loop between strand 3 and helix 3 of domain A, and domain C is a C-terminal extension characterized by a Greek key motif. The majority of these enzymes have an active site cleft between domains A and B, where a triad of catalytic residues (Asp, Glu and Asp) performs catalysis [6, 7].

Cold-active amylolytic microorganisms produce cold-adapted amylases, which function effectively at low temperatures. These cold-adapted enzymes exhibit high rates of catalysis in comparison with amylases from mesophiles or thermopiles, which exhibit little or no activity at low temperatures [1]. Therefore, cold-adapted α-amylases have emerged as one of the prime biocatalysts with broad potential in industrial applications, such as additives in processed food, in detergents for cold washing, in waste-water treatment, in bioremediation in cold climates and in molecular biology applications [7].

The ability to predict the tertiary structure of proteins has developed with computer technology and the increasing number of experimentally determined protein structures. Models created by homology modelling are often used to explain functions and characterizations. Comparing sequence information from newly isolated genes of naturally occurring organisms with genes of homologous enzymes with similar folding and function but different properties permits the identification of the molecular determinants and amino acid residues involved in the desired features. The recent and growing amount of available structural data on cold-active enzymes has prompted a detailed structural comparative analysis that provided new insights into the understanding of their molecular adaptations [8]. At present, many cold-adapted amylases have been reported from polar microorganisms, including *Alteromonas haloplanctis* [9], *Pseudoalteromonas haloplanktis* [8] and *Nocardiopsis* sp. 7326 [10]. To our knowledge, this is the first study on the sequence and structural characterization of a cold-adapted α-amylase of yeast origin.

In the present study, we isolated the encoding gene sequence of an α-amylase produced by *Glaciozyma antarctica* PI12. We also describe the enzyme properties based on sequence alignment and homology modelling. This study provides the first information on the structure and sequence of an amylase-encoding gene from the *G. antarctica* PI12 strain.

Materials and methods

Microorganisms, plasmids, growth media, enzymes and reagents

The psychrophilic yeast *G. antarctica* PI12 was obtained from the School of Biosciences and Biotechnology, Universiti Kebangsaan Malaysia, Malaysia. *Escherichia coli* JM109 (Promega, Madison, WI) was used as a cloning host. *G. antarctica* PI12 was grown on yeast extract peptone dextrose (YPD) and yeast extract peptone starch (YPS) [1 % (w/v) yeast extract, 2 % (w/v) peptone and 1 % (w/v) starch], both containing 25 μg/ml ampicillin and 25 μg/ml kanamycin. The *G. antarctica* PI12 cells were incubated at 4 °C for 7–8 days. *E. coli* JM109 was grown in Luria Bertani (LB) medium with 100 μg/ml ampicillin as the selecting antibiotic. All other chemicals were of analytical grade and were obtained from Promega, Sigma (St. Louis, MO), Amresco (Solon, OH), Fluka (Buchs, Switzerland) or Merck (Darmstadt, Germany).

Genomic DNA and total RNA isolation

Genomic DNA was extracted using a rapid isolation of yeast DNA protocol [11]. *G. antarctica* PI12 was grown in YPD broth at 4 °C for 7 days. The purified DNA was dissolved in Tris EDTA (TE) buffer or deionized water and stored at −20 °C. Total RNA was extracted from *G. antarctica* PI12 using the method described by Sokolovsky et al. [12]. Briefly, *G. antarctica* PI12 was grown at 4 °C for 7 days in YPS broth. The RNA was purified and used immediately for cDNA synthesis or stored at −80 °C.

DNA walking and cDNA synthesis of the full-length α-amylase gene

Primers used in the PCR amplifications are listed in Table 1. The partial DNA fragment of *G. antarctica* PI12 α-amylase was amplified using the primers AmyF and AmyR and *Taq* DNA polymerase (Promega), following the manufacturer's recommended protocol. The primers were designed based

Table 1 PCR primers used in this study

Primer name	Sequence (5′-3′)	Orientation	Use
AmyF	ATCTCGTCGCGCTGGACTCTGC	Forward	PCR
AmyR	CATCCTCGCCATCGTGACGGTC	Reverse	PCR
TSP 1-F	TCACCCTAACTGCGTCGGA	Forward	DNA Walking
TSP 1-R	CCCGTTCTTCTTCGCCTC	Reverse	DNA Walking
TSP 2-F	CGTCATTTGTAACGGCTCGGA	Forward	DNA Walking
TSP 2-R	CTTGGTCCTCTTGCCACCCTTG	Reverse	DNA Walking
TSP 3-F	TGGGGTGGTCGCAGGGGA	Forward	DNA Walking
TSP 3-R	CGAGGTCATAGAGGTCCTGCGTT	Reverse	DNA Walking
RTamyF	ATGGCCAACGACTCGACTC	Forward	RT-PCR
RTamyR	CTACTGCTTCCCGAATTCCTCC	Reverse	RT-PCR

on the Genome Sequencing Survey (GSS) Database of *G. antarctica* PI12, which is available from the Malaysia Genome Institute (MGI). The resulting DNA fragment was used to design primers for a subsequent DNA walking amplification to obtain the full-length AmyPI12 sequence. A DNA Walking SpeedUp Premix Kit (Seegene, Seoul, Korea) was used for the DNA walking amplification of AmyPI12, following the manufacturer's recommended protocol. Next, 5′-DNA walking was performed using the primers TSP 1-R, TSP 2-R and TSP 3-R, whereas 3′-DNA Walking was performed using the primers TSP 1-F, TSP 2-F and TSP 3-F. Augustus software [13] was used to predict introns. Using the sequence information from the DNA walking results, the full-length amylase gene was amplified using the primers RTamyF and RTamyR via RT-PCR. The DNA sequences amplified by PCR were confirmed by nucleotide sequencing (First BASE Laboratories, Seri Kembangan, Malaysia).

Data mining and sequence analysis

The resulting amino acid sequence (529 residues) was subjected to various sequence analyses with NCBI-BLAST [14], PSI-BLAST [15], ProtParam [16] and SignalP [17], whereas Interproscan and SUPERFAMILY HMM [18] were used to identify any possible families or conserved domains in the protein. The multiple sequence alignment of the AmyPI12 sequence with other proteins was performed using ClustalW [19].

Phylogenetic analysis of AmyPI12

The phylogenetic relationship of AmyPI12 was generated using 37 other deduced α-amylases available from the NCBI databases, as shown in Table 2. A phylogenetic tree was constructed by multiple sequence alignment using Clustal X [20] and the neighbour-joining (NJ) method and bootstrap analysis. The phylogenetic tree was visualized using the Treeview software. The confidence values for the individual branches were assessed from 1,000 bootstrap replicates of the original sequence data.

Molecular model building

The template search and secondary structure prediction for AmyPI12 were conducted using the BLAST-PDB [14], phyre [21], HHPRED [22] and Modlink+ [23] programs. The structure of AmyPI12 was predicted by homology modeling based on the crystal structure of *Bacillus stearothermophilus* (BSTA) α-amylase (1HVX) using MODELLER9.9 [24]. This program is an automated approach to comparative modeling via satisfying spatial restraints. The modeling procedure begins with the alignment of the sequence to be modeled (target) with related known three-dimensional (3D) structures sequences (templates). A hundred models were generated, and the model with the lowest objective function value was selected for further analysis. Optimization and energy minimization of the resulting models was performed using the steepest descent algorithm implemented in GROMOS from Deepview [25].

Validation and assessment of the homology model

To assess the reliability of the modelled structure of AmyPI12, model quality was assessed by the geometry quality of the backbone conformation, the residue interaction, the residue contact and the energy profile of the structure using different methods, including PROCHECK [26], ERRAT [27], PROSA-WEB [28] and VERIFY 3D [29, 30].

Results and discussion

Cloning and sequence analysis of AmyPI12 from *G. antarctica* PI12

A nucleotide sequence from the *G. antarctica* PI12 genome obtained from a GSS database was identified as encoding

Table 2 α-Amylase from different organisms used in the phylogenetic analysis

Taxanomy	Name/source	Abbreviation	Accession No
Eukaryota			
Fungi			
Dikarya			
Basidiomycota			
Pucciniomycotina	*Glaciozyma antarctica* PI12	*G.antarctica*	JX839765
	Melampsora larici-populina	*M.larici*	EGG10518.1
Agaricomycotina	*Cryptococcus neoformans*	*C.neoformans*	XP_572173.1
	Cryptococcus gattii	*C.gattii*	XP_003195041.1
	Auricularia delicata	*A.delicata*	EJD53851.1
	Stereum hirsutum	*S.hirsutum*	EIM80671.1
	Dacryopinax sp.	*Dacryopinax*	EJU02147.1
	Trichosporon asahii	*T.asahii*	EJT45014.1
	Piriformospora indica	*P.indica*	CCA68317.1
Ascomycota			
Pezizomycotina	*Zymoseptoria tritici*	*Z.tritici*	XP_003854737.1
	Leptosphaeria maculans	*L.maculans*	XP_003843104.1
	Cordyceps militaris	*C. militaris*	EGX87928.1
	Glomerella graminicola	*G.graminicola*	EFQ35156.1
	Verticillium dahliae	*V. dahliae*	EGY16551.1
	Verticillium albo-atrum	*V.albo*	XP_003004668.1
	Colletotrichum higginsianum	*C. higginsianum*	CCF46315.1
	Pyrenophora tritici-repentis	*P.tritici*	XP_001940506.1
	Magnaporthe oryzae	*M.oryzae*	XP_003716674.1
	Neurospora crassa	*N.crassa*	CAE75731.1
	Aspergillus oryzae	*A.oryzae*	XP_001820541.2
	Aspergillus flavus	*A.flavus*	XP_002373860.1
	Exophiala dermatitidis	*E.dermatitidis*	EHY55318.1
Bacteria			
Firmicutes			
Bacillales	*Paenibacillus* sp.	*Paenibacillus*	ZP_08281424.1
	Bacillus circulans	*B.circulans*	CAA43194.1
	Paenibacillus lactis	*P.lactis*	ZP_09000645.1
	Bacillus coagulans	*B.coagulans*	YP_004859330.1
	Macrococcus caseolyticus	*M. caseolyticus*	YP_002559717.1
Lactobacillales	*Carnobacterium* sp.	*Carnobacterium*	YP_004373784.1
	Carnobacterium sp.	*Carnobacterium*	ZP_02185357.1
Clostridia	*Anaerococcus vaginalis*	*A.vaginalis*	ZP_05471910.1
	Anaerococcus hydrogenalis	*A.hydrogenalis*	ZP_08170295.1
	Clostridium sticklandii	*C. sticklandii*	YP_003935087.1
Negativicutes	*Pelosinus fermentans*	*P.fermentans*	ZP_10328301.1
Verrucomicrobia			
Verrucomicrobiae	*Akkermansia muciniphila*	*A.muciniphila*	YP_001878411.1
Bacteroidetes			
Bacteroidia	*Parabacteroides distasonis*	*P.distasonis*	YP_001302321.1

part of an α-amylase gene sequence using NCBI-BLAST databases. Isolation of the full-length α-amylase gene was accomplished by DNA walking, followed by RT-PCR amplification. A DNA fragment of approximately 1,700 bp was obtained using PCR. Due to lack of DNA sequence information on the *G. antarctica* PI12 α-amylase, DNA walking techniques were used to amplify the full-length DNA sequence. The DNA walking method was conducted using the

DNA of *G. antarctica* PI12 and the 5′- and 3′-portion sequences of the full-length DNA were obtained by 5′- and 3′-DNA walking, respectively. Approximately 700 bp was amplified using 5′ RACE, and approximately 650 bp was amplified using 3′ RACE. Conjugation of the 5′ and 3′ fragments revealed a full-length α-amylase DNA sequence of 3,035 bp containing a 529-bp ORF, a 124-bp 5′ untranslated region and a 519-bp untranslated flanking region at the 3′ end. An analysis of the full-length DNA sequence encoding the α-amylase from *G. antarctica* PI12 using Augustus software revealed 15 introns flanking the exon sequence. Based on this finding and the DNA walking sequences, a set of primers was designed (RTamyF and RTamyR), and the full-length cDNA sequence (1,590 bp) was amplified using the RT-PCR method. The full-length DNA sequence of the *G. antarctica* PI12 α-amylase was deposited with GenBank under the accession no. JX839765.

The 1,590-bp cDNA sequence of *G. antarctica* PI12, known as AmyPI12, encodes a 530-amino acid protein with a calculated molecular weight of 59.7 kDa and a theoretical pI of 4.8. SignalP [17] prediction revealed that the AmyPI12 protein contains no putative signal peptide, which suggests that this enzyme is involved only in the intracellular mechanism of *G. antarctica* PI12. Interproscan [31] analysis predicted that AmyPI12 encodes a glycosyl hydrolase family 13 member because it contains a conserved catalytic domain observed in several protein members of this family. In addition, the conserved domain search from CDD analysis [32] indicated that AmyPI12 from *G. antarctica* PI12 has an α-amylase catalytic domain observed in bacterial and fungal α-amylases. Based on a Blast search analysis, the AmyPI12 amino acid sequence was determined to be 66 % and 64 % identical to the sequence of α-amylase from *Cryptococcus neoformans* and family 13 glycoside hydrolase from *Melampsora larici-populina*, respectively.

Phylogenetic analysis of AmyPI12

To investigate the evolutionary relationships among the cold-adapted α-amylase identified in this work (AmyPI12) and others reported in the literature, a phylogenetic analysis was performed. The search for a complete protein sequence was explored using the NCBI BlastP service. A total of 34 α-amylase sequences, as shown in Table 2 (all hits with an e-value lower than 6×10^{-150}), were downloaded and aligned using Clustal X. From this alignment, a NJ tree was constructed to examine the distances among these sequences. The NJ tree was then inferred, and the tree topology was analyzed using bootstrapping (1,000 replicates). The probable alpha-amylase of *Ustilago hordei*, which did not coincide with the taxonomic status of the AmyPI12, was used as an out-group to root the tree.

The analysis summarized in Fig. 1 shows that the α-amylase sequences clustered into two supported subgroups corresponding to clade I and II, which are both monophyletic clades. The monophyletic lineages provide support for the hypothesis that the clade I and II α-amylases are likely to have evolved from one common ancestor [33]. The α-amylases from Ascomycota were clustered and formed subclade Ia, whereas α-amylases from the bacteria domains Firmicutes, Verrucomicrobia and Bacteroidetes were clustered and formed subclade Ib. α-Amylase from Basidiomycota were clustered and formed the second monophyletic clade, clade II.

The AmyPI12 α-amylase from *G. antarctica* PI12 was clustered in the Basidiomycota group. Homology values ranging between 66 % and 60 % were observed when comparing AmyPI12 with the other Basidiomycota α-amylases. Bootstrap values, which comprise an index of the accuracy of the phylogenetic tree, were found to be higher outside the tree but lower inside the tree, which may indicate the low relative diversity of all the sequences used in the analysis [34]. Orikoshi et al. [35] suggested that the redundancy of the genes within the same species may reflect their functional difference between related proteins and also the adaptive evolution of the genes.

Three-dimensional model of AmyPI12

To elucidate and understand characteristics of the α-amylase, a model of the 3D structure of AmyPI12 was constructed. A template search against the BLAST-PDB, phyre, HHPRED and Modlink+ databases revealed various potential templates for molecular modelling purposes. Among them, a crystal structure of BSTA α-amylase (PDB ID: 1HVX), which had the highest sequence identity (47 %), was selected as a template. To further assess the reliability of the structural sequence alignment between AmyPI12 and 1HVX, consensus secondary structure prediction was used to confirm the alignment. This was achieved by comparing the aligned secondary structure of 1HVX and the consensus predicted secondary structure of AmyPI12. The structural alignment indicated a good alignment of eight α-helices and nine β-strands between AmyPI12 and 1HVX. The rest of the protein regions were shown to consist of random coils and a few structural mismatches and gap-containing segments.

The alignment results between AmyPI12 and 1HVX were used to build models with MODELLER. MODELLER is a program that works based on the satisfaction of spatial restraints. The program satisfies all the restraints derived from the structure-sequence alignment. Models that produced high violations of the restraints were considered poor, and those models led to higher objective functions, such as by the CHARM-22 force field [36]. The model with the lowest objective function was then selected. The resulting model was subjected to energy minimization using the

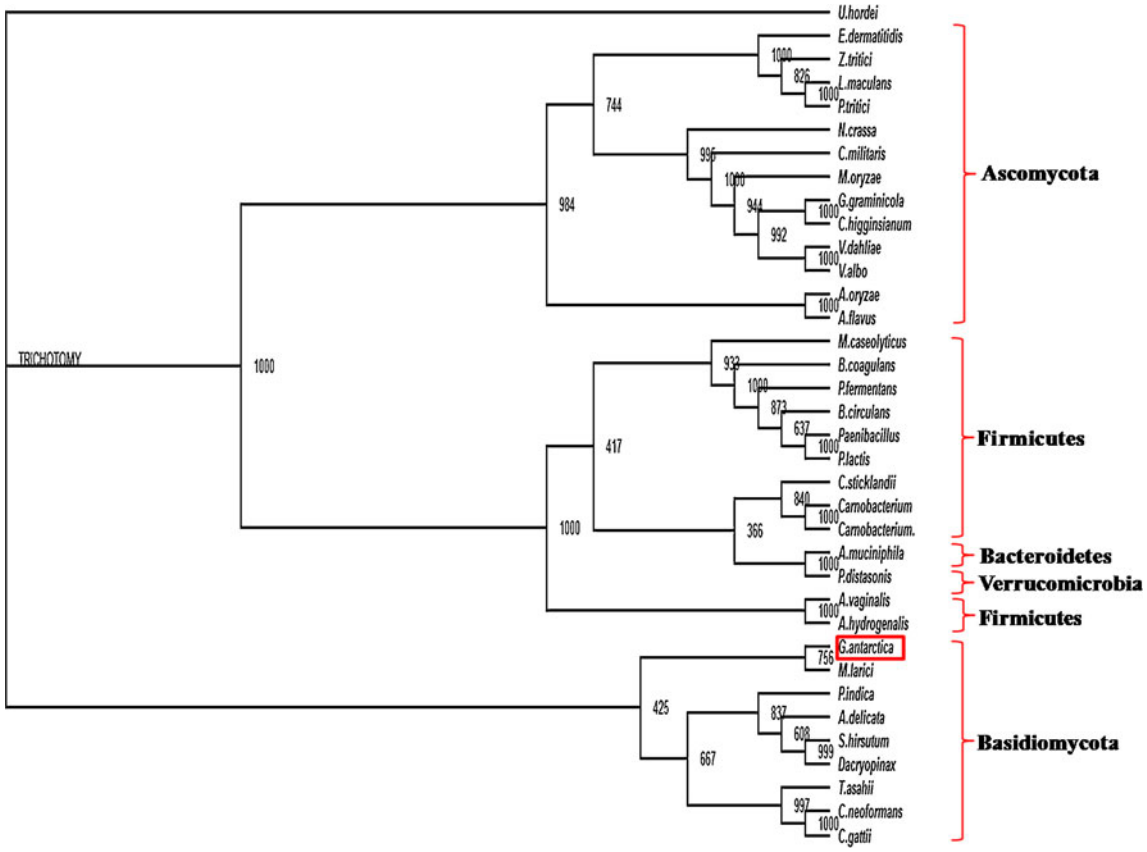

Fig. 1 Phylogenetic tree showing the relationship between AmyPI12 from *Glaciozyma antarctica* PI12 and other α-amylases. The α-amylase gene of *Ustilago hordei* was used as an out-group to root the tree. The confidence values were assessed from 1,000 bootstrap replicates of the original sequence data

steepest descent algorithm as implemented in GROMOS from Deepview to avoid poor molecular contacts.

Model validation and assessment

The quality of the refined model was evaluated using PROCHECK, VERIFY3D, ERRAT and ProSA-web. The PROCHECK program was used to measure the residue-by-residue stereochemical quality of the AmyPI12 model to construct a Ramachandran plot [26]. In structure validation, Ramachandran plots are often used to visualize the backbone dihedral angles ψ against φ of amino acids in a protein structure [37]. The plot of the AmyPI12 model indicated that only two residues were located in the disallowed region (Tyr149 and Ala186); 88.9 % of the residues were located in the most favoured region, and the remaining residues resided in the additional and generously allowed regions. The VERIFY3D program was used to determine the compatibility of an atomic model (3D) with its own amino acid sequence (1D) by assigning a structural class based on its location and environment and comparing the results to good structures [29, 30]. The VERIFY3D analysis indicated that 92.09 % of the residues had an average 3D–1D score greater than 0.2, indicating that only 7.91 % of the residues did not complement the 3D–1D profile. A VERIFY3D score of greater than 80 % indicates that the predicted model is of satisfactory quality [30]. The ERRAT program examines the overall quality factor for non-bonded atomic interactions. Scores of 50 % and higher are normally acceptable and indicate a high-quality model [27]. The ERRAT score for the AmyPI12 model was 83.667 %, suggesting that the backbone conformation and non-bonded interactions of the model are all reasonable within a normal range. In addition, model assessment was performed using ProSA-web to calculate an overall quality score for a specific input structure. If this score is outside a range that is characteristic for native proteins, the structure most likely contains errors. The z-score of the input model (AmyPI12) was determined to be −7.78, indicating that this model is within the range for native proteins. It also indicates that this homology model is consistent with reliable conformation based on its similarity [28]. Based on the validation and assessment, a reasonable predicted model of AmyPI12 was constructed. The geometric quality of the backbone conformation, the residue interaction and the residue contacts of the structure were all well within the limits established for reliable structures.

AmyPI12 model analysis

The final and validated AmyPI12 model is shown in Fig. 2. The general structure of the model is characterized by three distinct domains with overall topologies similar to those observed in all known structures of α-amylases and related amylolytic enzymes [5]. The largest domain, domain A, forms the core of the molecule. It consists of an eight-stranded parallel β-barrel surrounded by a concentric cylinder of α-helical segments, known as a $(\beta/\alpha)_8$ barrel structure, and comprises residues 1–102 and 207–394. A second domain, domain B, is the least similar domain in α-amylases. In AmyPI12, domain B becomes a complex multi-strand domain with over 100 residues compared with a relatively short (~60 residues) loop-like structure with little regular secondary structure in the α-amylases from *Aspergillus oryzae* [38] and psychrophilic α-amylases from *Alteromonas haloplanctis* [9]. Domain B was established as a protrusion from domain A and was built from residues 103–206. Domain B of AmyPI12 is characterized by two long central β-strands (residues 112–118 of Bβ1 and residues 132–136 of Bβ2) that are wound around each other in a double-helical fashion. The C-terminal portion of the longer strand is capped by a shorter antiparallel strand (residues 160–162 of Bβ3). Another antiparallel β-strand is located underneath the central portion of the long strand (residues 174–176 of Bβ4). An α-helix (Bα1) is likely involved in forming the extended substrate binding site is present in AmyPI12 but is shorter compared with the helix in barley α-amylase [39]. To compensate for this, AmyPI12 contains a pronounced loop (Fig. 2) that is wound around the Ca-Na-Ca metal triad and may be involved in binding the substrate [40]. The ligands for the Ca-Na-Ca metal triad come almost completely from the residues in domain B, with only some interactions established with residues from domain A. The unique characteristics of domain B for cold adaptation in low temperatures are discussed in the section on Structural determinants specifying the flexibility in *G. antarctica* PI12 α-amylase, AmyPI12. Domain C forms a β-barrel structure (consisting of eight β-strands) containing a Greek key motif [41]. This domain is generally well conserved in amylolytic enzymes except in barley [9] and human salivary α-amylases [39], where it is significantly smaller (consisting of only five β-strands) and larger (consisting of ten β-strands), respectively.

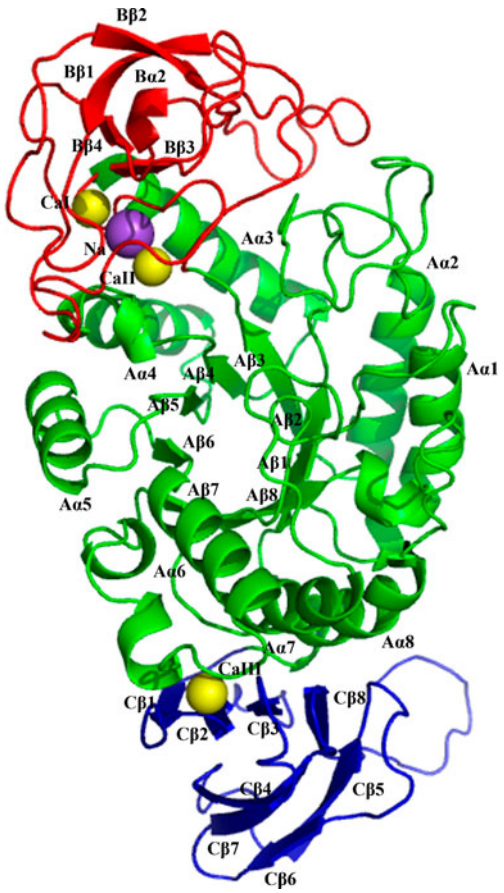

Fig. 2 A 3D model of AmyPI12. *Green* Domain A, *red* domain B, *blue* domain C. The α-helices and β-strands in domain A are labelled Aα1–Aα8 and Aβ1–Aβ8, respectively, whereas in domain B are labelled Bα1 and Bβ1–Bβ4, respectively. The β-strands in domain C are labelled Cβ1–Cβ8. *CaI*, *CaII*, *CaIII* predicted calcium ions, *Na* sodium ion

AmyPI12 also possesses all three important residues at the active site (Asp232, Glu263 and Asp330) that play crucial roles in the chemical catalysis as general acid/base catalysts or in substrate binding [42]. In a proposed bond cleavage mechanism, the glycosidic oxygen is initially protonated by a general acid catalyst, Glu263—one of three invariant carboxylic acid residues at the catalytic site of AmyPI12. The C1 of the substrate glycan part is attacked by a nucleophile Asp232 and a third carboxylate group Asp330 presumably activates the water, hydroxylating at C1, stabilizing the oxycarbenium ion-like transition state and helping maintain the glutamic acid in the correct state of protonation for activity [43]. Those three residues occurring in AmyPI12 are crucial for the reaction process because replacing any of the residues leads to an essential loss of activity [44]. The active site is situated at the bottom of the substrate binding cleft, which is positioned at the interface between the $(\beta/\alpha)_8$-barrel and the extended loop. The residues in the active site are strictly conserved.

The superimposition of the 3D AmyPI12 model with the structure of 1HVX (Fig. 3a) yielded a root mean square deviation (RMSD) of 0.254 Å that covered 97.3 % of the backbone atoms, indicating a good overall structural alignment. The proposed catalytic residues for the modelled AmyPI12 structures (Asp232, Glu263 and Asp330) are represented as ball and sticks and fall into approximately the same locations as in 1HVX (Fig. 3b). The conservation of the catalytic residues and the identical structural assignments in the modelling suggest that the modelled α-amylase

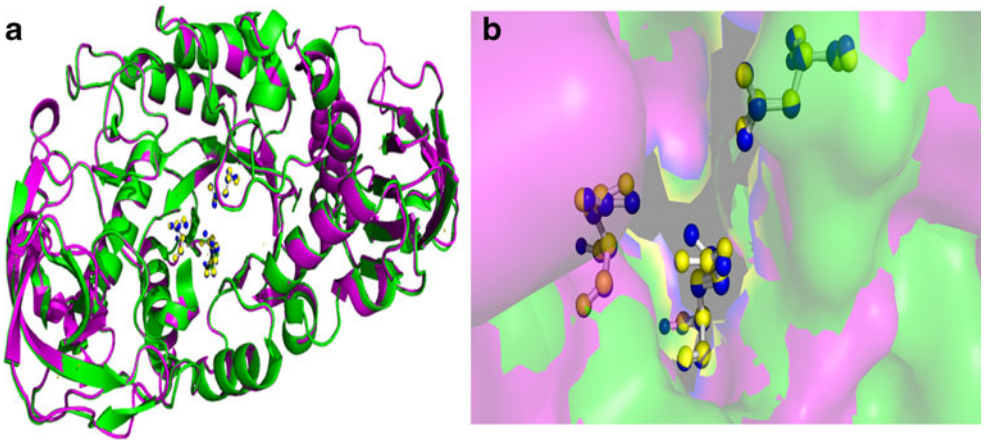

Fig. 3 **a** Superimposition of the refined AmyPI12 model and its template, 1HVX. Both structures are shown in cartoon representation. *Green ribbon* 1HVX structure, *magenta ribbon* AmyPI12 model. The catalytic regions of both models are represented as *balls and sticks*. **b** Close-up view of AmyPI12 catalytic residues (*blue*; Asp232, Glu263 and Asp330) compared with 1HVX catalytic residues (*yellow*; Asp234, Glu264 and Asp331)

structure (AmyPI12) is an accurate representation of the actual protein structure (1HVX).

The α-amylases are classical calcium-containing enzymes. A calcium ion is present at the location homologous to the common calcium-binding sites in α-amylases [45]. In AmyPI12 (Fig. 2), the conserved calcium ion is designated as calcium I (CaI); the second as calcium II (CaII); and the third, which is rarely observed in structure of amylolytic enzymes and conserved in certain *Bacillus* α-amylases, as calcium III (CaIII). Generally, CaI and CaII are in close proximity to a central cation, sodium (Na), that is known to have stabilizing and activating effects on some α-amylases [5, 45]. The third calcium ion, CaIII, is located in the interface between domains A and C. This calcium ion, which was first observed in the thermostable *Bacillus licheniformis* (BLA) α-amylase and is responsible for bridging two loops in domain C with a large loop in domain A, has been suggested to be involved in the increased thermostability [5]. The positions of the ion-binding sites for CaI, CaII, CaIII and Na were identified by alignment of the AmyPI12 model with the 1HVX structure liganded with all of these ions.

The conserved calcium ion CaI is liganded by four residues in all the structures of amylolytic enzymes [5, 42, 45]. As shown in Fig. 4a, three of these residues are strictly conserved in AmyPI12 and could be identified as Asp195, Asp201 and His236 by a structure-based sequence alignment with its template 1HVX, which is the thermostable α-amylase from BSTA. These three residues were also observed to interact with the central sodium ion (Na). The fourth ligand, Asn103, is not conserved and could not be deduced from sequence comparisons; however, this residue also binds to CaI (Fig. 4a). A previous study by Machius et al. [5] reported that calcium binding of CaI controls the formation of the extended substrate binding site, thus explaining on a structural level how the calcium ion activates α-amylases and related amylolytic enzymes.

Whereas CaI is essential for maintaining the proper configuration of the active site residues, the non-conserved calcium (CaII and CaIII) and sodium (Na) ions are suggested to confer extra thermostability of thermostable α-amylases by delaying the thermally induced unfolding of domain B and the subsequent disorganization of the catalytic region [40]. The presence of these non-conserved calcium and sodium ions in cold-adapted AmyPI12 is unexpected because AmyPI12 exists at opposite temperatures and tends to be thermolabile. However, as shown in Fig. 4b, the ligands binding CaII in AmyPI12 are different from those in 1HVX except for Asp205 (equivalent to Asp203 in AmyPI12). The ligand residues of Asp162, Ala184 and Asp186 in 1HVX are replaced with Thr160, Ser182 and Ala184 in AmyPI12, and only two of these three residues (Thr160 and Ala184) bind to CaII. These results clearly suggest that the CaII in cold-adapted α-amylases appear to be more loosely held, as judged from the temperature factors of AmyPI12. A previous study of cold-adapted α-amylases from *A. haloplanctis* for calcium affinity demonstrated a lower affinity for this ion in comparison with mesophilic α-amylase, as reflected by a 10^4 higher dissociation constant [46].

Sodium becomes a central cation with close proximity to the two calcium ions of CaI and CaII. A specific sodium-binding site in an α-amylase was first described in the thermostable α-amylases of BLA [5]. It has been known for some time that sodium enhances the stability and enzymatic activity of some α-amylases [47]. Based on the structure–structure alignment (Fig. 4c), Na is liganded by five residues in AmyPI12, in which one of these residues binds CaI (Ala184) and two of these residues bind CaII (Asp195 and Asp201). The other two residues of Asp162 and Leu204 in 1HVX are replaced by Thr160 and Ile202, respectively, which exhibit no binding to the Na ion. This observation also suggested that the low Na affinity of AmyPI12 leads to the low stability of AmyPI12, allowing it to work at different temperature scales.

The third calcium ion, CaIII, in AmyPI12 is located in the interface between domains A and C. This calcium ion bridges a loop in domain C (Tyr304, Glu305) with a large loop in domain A (Pro405 and Asn406), whereas in 1HVX, the

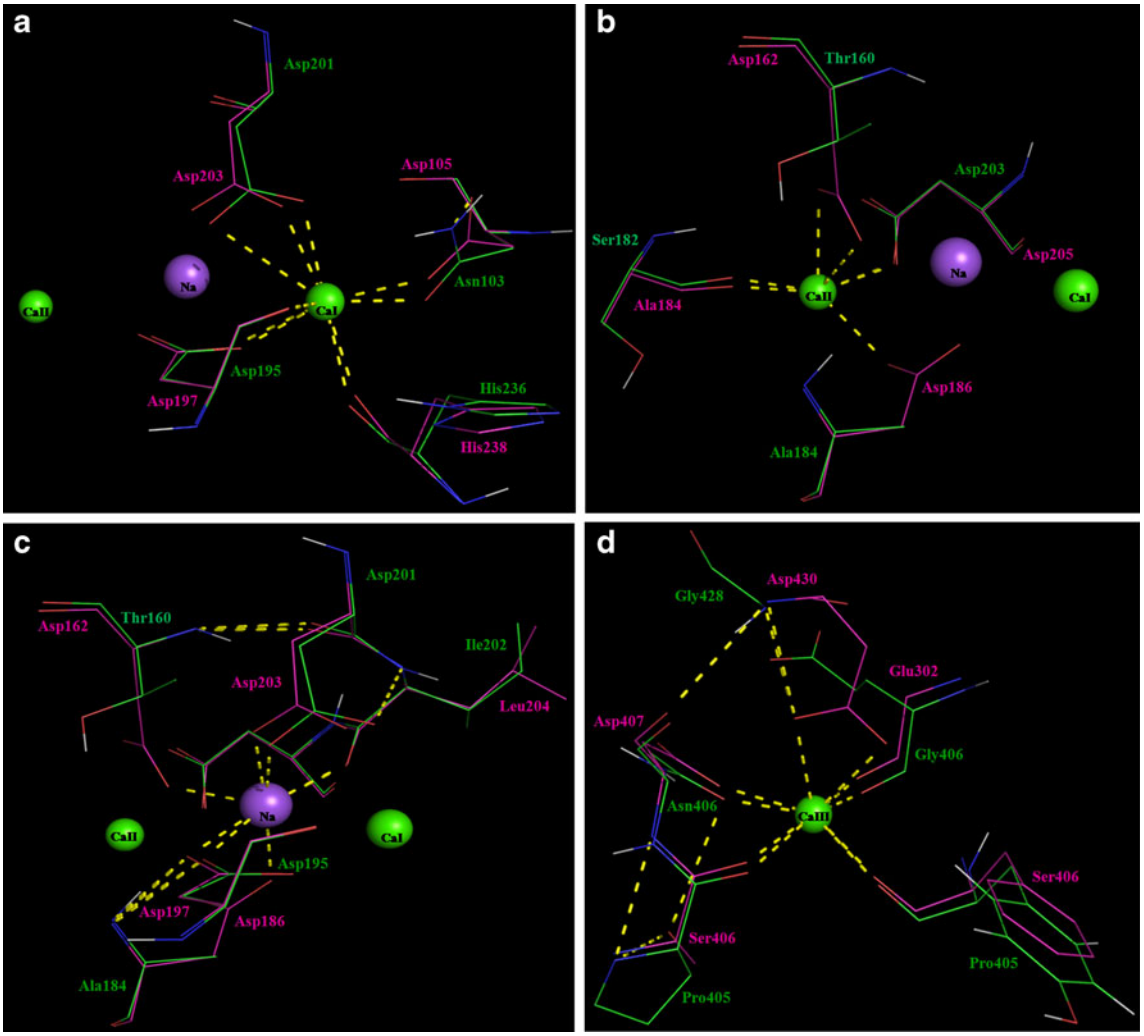

Fig. 4 **a**–**d** Superimposition of the ligand residues involved in the metal binding of AmyPI12 (*green*) and 1HVX (*magenta*). Ligand residues involved in CaI- (**a**), CaII- (**b**), Na- (**c**) and (**d**) CaIII-binding are shown

CaIII bridges two loops in domain C with a large loop in domain A (Fig. 4d). This demonstrates the low affinity of AmyPI12 toward CaIII, thus suggesting the low stability of this cold-adapted enzyme that leads to increased flexibility at low temperatures because CaIII is also involved in the stability of the α-amylases.

Structural determinants specifying flexibility in *G. antarctica* PI12 α-amylase, AmyPI12

The sequence–structure comparison of AmyPI12 revealed the highest identity (47–46 %) to the solved crystal structure of liquefying α-amylase from BSTA, BLA, *Bacillus halmapalus* (BHA), *Bacillus* sp. 707 (SPA) and *Bacillus amyloliquefaciens* (BAA). Interestingly, all the solved crystal structures of α-amylases that display the closest identity to AmyPI12 are thermostable proteins. Considering this high structural identity of AmyPI12 with thermophilic α-amylases, it has been suggested that the structural adaptation of psychrophilic enzymes to low temperatures may be similar to that of thermophilic enzymes to high temperatures. However, the distinctive thermolability and psychrophilicity presumably reflect the structural differences in an opposite manner [48]. Previously, Schlatter et al. [49] and Vckovski et al. [50] reported that psychrophilic lactate dehydrogenase (LDH) shares more homology with thermophilic LDH than with mesophilic LDH, which indicates that psychrophilic enzymes appear, to some extent, to have similar structural adaptations to low temperatures as thermophilic enzymes have to high temperatures. The structural comparison involved in the cold-adaptation analysis of AmyPI12 was made with only two of these five solved crystal structures—BSTA and BLA—for which thermostability adaptations have been determined and well-studied previously.

The most variable domain in α-amylases is domain B. This domain is an extrusion from domain A and is located between Aα3 and Aβ3 of AmyPI12 (Fig. 2). Domain B is absent in saccharifying α-amylases such as *B. subtilis* α-amylases

(BsuA) [51], whereas in liquefying bacterial α-amylases such as BSTA [45] and BLA [40], the domain has striking features and is elongated by up to 100 residues [52]. The folding of domain B over the top of the $(\beta/\alpha)_8$ barrel of domain A forms a cleft that contains the extended primary substrate-binding site and the active site as shown in Fig. 5. Joyet et al. [53] and Declerck et al. [40] reported that domain B and its interface in domain A are particularly sensitive to any structural perturbation such that any mutation altering or reinforcing stabilizing interactions in this region may considerably decrease or increase the rate of thermal inactivation. Therefore, it has been suggested that the overall thermostability of thermostable α-amylases concentrate in domain B, and their interfaces concentrate within the central A domain.

Based on the high similarity of AmyPI12 to thermostable α-amylases (BSTA, BLA, BHA, SPA, BAA), it has been suggested that domain B and its interface with the central A domain became the main target for cold-adaptation of AmyPI12 to facilitate survival in low-temperature environments. This structural adaptation is assumed to be opposite from the high-temperature adaptations in thermophilic enzymes. It has been reported that the increased thermostability of BLA is associated with shortening of the loop region in the vicinity of the active site and located in domain B (equivalent to residues 178–199) after the β-strand Bβ4, which improves the calcium binding of BLA. In contrast, this loop region is lengthened in AmyPI12 by up to 29 residues (at positions 177–206 of AmyPI12), which suggests that the flexibility of this region allows it to function at different temperature scales. Furthermore, it was revealed that two residues of the thermostable α-amylase of BLA, equivalent to residues Asp183 and Glu185, were replaced by smaller residues of alanine (at the equivalent positions of 184 and Ala186, respectively) in AmyPI12. It has been suggested previously that, to attain sufficient activity at low temperatures and facilitate substrate binding, the active site cleft of cold-adapted enzymes are larger and more accessible to the substrate. This type of architecture is achieved by replacing amino acids that have bulky groups with those that have smaller side chains and by increasing the length of loops around the active site [54]. The loop structures around the active sites have previously been reported to have enhanced flexibility, resulting in increased K_m [55]. In addition, the shortening of loops and turns is more frequently observed in thermophilic proteins than in their mesophilic counterparts [9]. In AmyPI12, this loop region contains four metal-binding residues (Asp186, Asp195, Asp201 and Ile 202) compared with the three in BLA α-amylase and at least two residues implicated in substrate binding (Glu190 and Met198), as shown in Fig. 5. Therefore, the proper configuration of this loop is crucial for enzyme structure and function [40].

In addition, an interesting study of thermostable α-amylases from BLA by Declerk et al. [40] can be used to explore the flexibility features of cold-adapted AmyPI12. Declerk et al. discovered several residues that were particularly intolerant to amino acid substitutions and led to mutants that were extremely unstable compared with the wild-type enzyme. These residues—Asn192, Asp204 and Lys237—in the sequence of BLA α-amylases were, surprisingly, substituted with other residues in AmyPI12, Ser193, Ser205 and Glu238, respectively (Fig. 6). All of these residues are clustered at the interface between the A and B domains, near the hinge where the

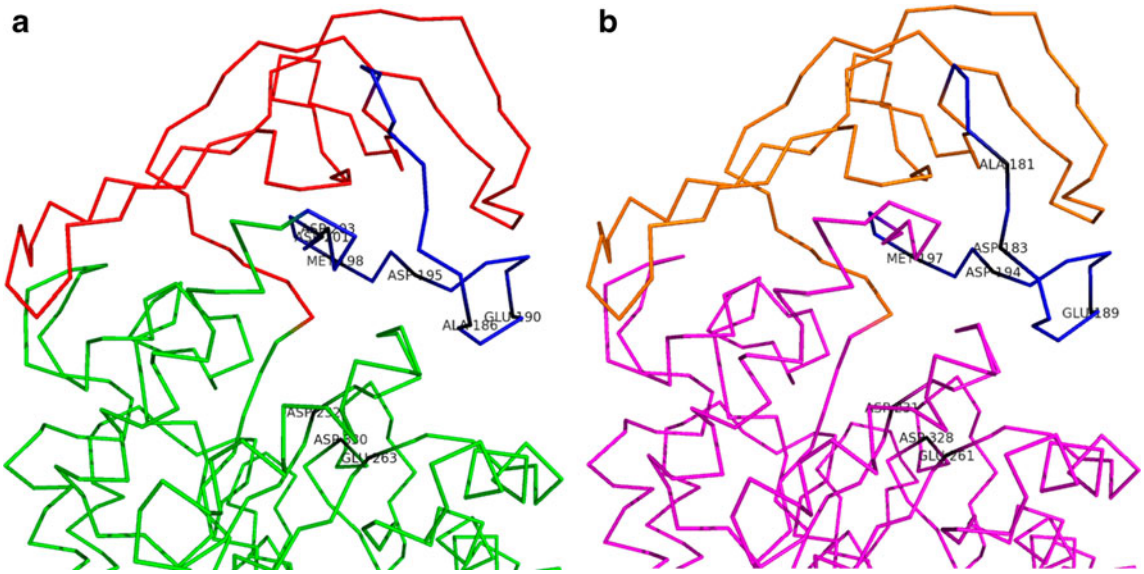

Fig. 5a,b Schematic representation of domain B over the top of domain A. **a** Ribbon model of AmyPI12 from *G. antarctica* PI12. *Green* Domain A, *red* domain B, *blue* spanning loop region. **b** Ribbon model of thermostable α-amylases from BLA. *Magenta* Domain A, *orange* domain B, *blue* spanning loop region. *Black* Metal-ligand residues implicated in substrate binding, and catalytic residues

conserved calcium binding site is located. In BLA, these polar residues are important for electrostatic interactions at this region and are thus a major stabilizing feature associated with the adaptation of BLA at extreme temperatures. However, in AmyPI12, the substitution with other less polar amino acids might reflect the loss of essential interactions and play a key role in the cooperative unfolding or refolding process of the polypeptide that leads to loss of stability. Therefore, this observation supports the notion that the decreased stability of AmyPI12 in cold environments leads to increased flexibility.

Examination of the psychrophilic characteristics of AmyPI12 using the amino-acid sequence alignment of psychrophilic (AmyPI12) and thermophilic (SPA, BHA, BSTA, and BLA) α-amylases indicated that the residues that are essential for α-amylase activity, particularly Asp232, Glu263 and Asp330, were also observed in the AmyPI12 catalytic domain, implying the crucial role of these residues in the catalytic activity and structure of α-amylases (Fig. 6). Previous research has shown that each cold-adapted enzyme uses different small selections of residue changes that result in structural adjustments. These adjustments typically increase the molecular flexibility, which, in turn, gives rise to increased catalytic efficiency and reduced stability in certain protein regions [3, 56]. The

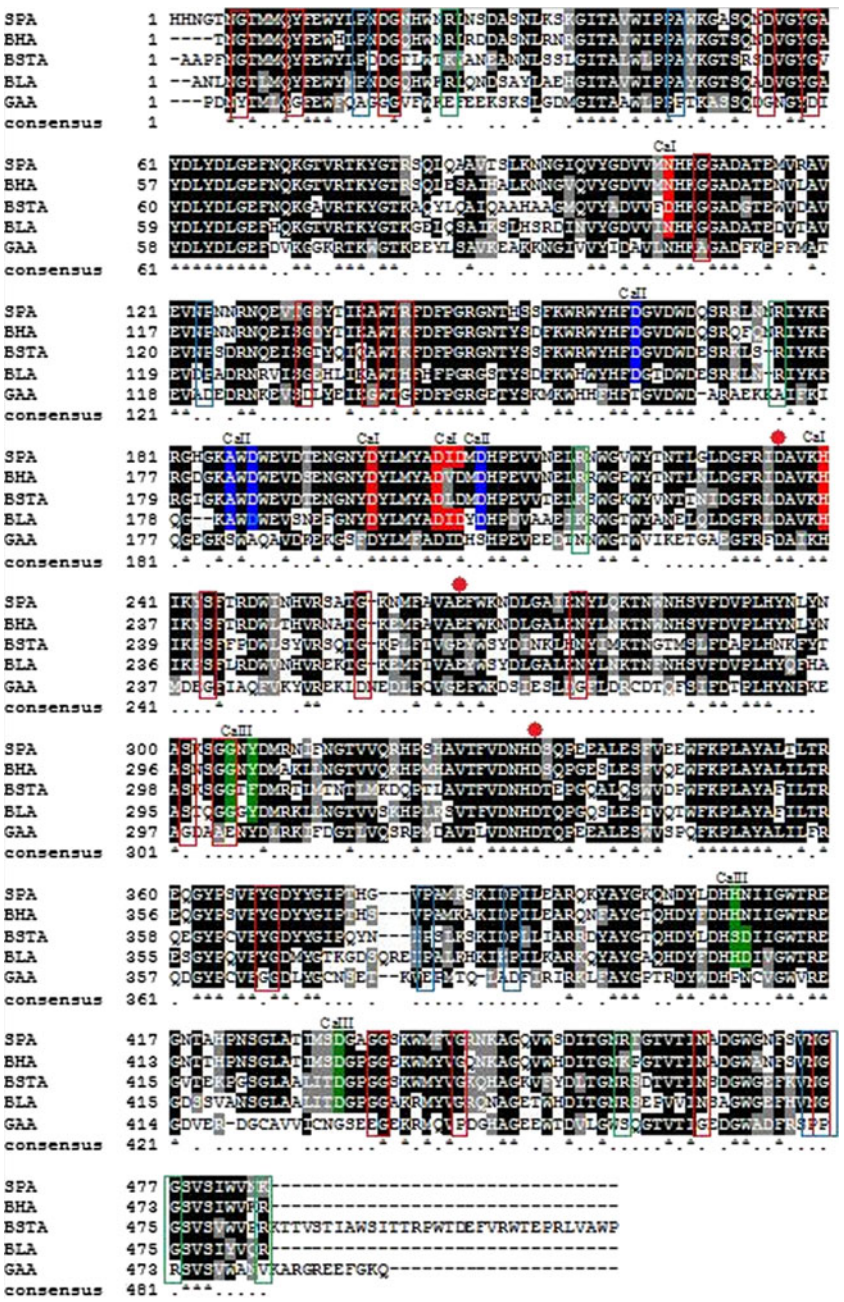

Fig. 6 Alignments of amino acid sequences of α-amylases from thermophiles: *Bacillus* sp.707 (SPA), *Bacillus halmapalus* (BHA), *Bacillus stearothermophilus* (BSTA), *Bacillus licheniformis* (BLA) and a psychrophile: *G. antarctica* PI12 (GAA). *Red dots* Conserved catalytic residues, Asp232, Glu263 and Asp330; *red boxes* glycine substitutions; *blue boxes* proline substitutions; *green boxes* arginine substitutions. The residues involved in calcium- and sodium-ion binding sites are indicated by CaI, CaII, CaIII and Na and highlighted by *red*, *blue* and *green* backgrounds, respectively

multiple sequence alignment of AmyPI12 with other thermophilic α-amylases in Fig. 6 revealed several interesting substitutions of the signature psychrophilic amino acid residues: proline, arginine and glycine. These substitutions are divided into two classes: flexibility substitutions and stability substitutions.

Glycine is thought to modulate the entropy of protein unfolding by affecting the flexibility of the backbone. The lack of a side chain in glycine allows chain rotations and dihedral angles not available to other residues. Clusters of glycine residues are thought to increase localized chain mobility [57]. Substitutions of amino acids with glycine occurred at positions 9, 17, 52, 136, 139, 240, 274, 298, 365 and 463 of AmyPI12, where thermophilic α-amylases have other residues, such as tyrosine, serine, alanine, asparagine, aspartate and the positively charged residues arginine, lysine and histidine, at structurally equivalent positions (Table 3). The stacking of glycine around the catalytic residues improves the flexibility of the active site [57]. Therefore, it has been suggested that the replacement by glycine at position 274 (Gly274) in AmyPI12 may contribute to the high catalytic efficiency of AmyPI12 at low temperatures. In addition, Feller et al. [58] suggested that the occurrence of glycine clusters close to functional domains is also related to structural flexibility. The replacement by glycine clusters was observed at positions 17 and 365 of AmyPI12 likely provides local mobility to the functional domain of this enzyme.

Table 3 Amino acid substitutions in AmyPI12 compared with the equivalent locations in mesophilic and thermophilic α-amylases. The comparison and analysis were performed based on the amino acids sequence alignment in Fig. 6

Type of substitution	Amino acid involved	Residue in psychrophilic AmyPI12	Residue in thermophilic α-amylases
Flexibility	Glycine	Gly9	Tyr
		Gly17	Asp
		Gly52	Asp
		Gly136	Ala
		Gly139	Arg, Lys, His
		Gly240	Ser
		Gly274	Asn
		Gly298	Ser
		Gly365	Tyr
		Gly463	Asn
	Proline	Ala5	Pro
		Asp121	Pro
		Glu378	Pro
		Asp385	Prol
	Arginine	Glu23	Arg
		Ala172	Arg
		Asn214	Arg, Lys
		Val481	Arg
Stability	Proline	Pro44	Ala
		Pro439	Gly
		Pro471	Asn
		Pro472	Gly
		Pro474	Gly
	Glycine	Tyr4	Gly
		Asp56	Gly
		Ala106	Gly
		Asp130	Gly
		Asp254	Gly
		Ala301	Gly
		Glu302	Gly
		Glu431	Gly
	Arginine	Arg475	Gly

Proline is an imino acid, as its side chain is covalently linked to its backbone. The pyrolidine ring of proline severely restricts the possible conformations of the preceding residue. Proline is believed to decrease the backbone entropy of unfolding by constraining the main-chain flexibility, which consequently increases both the protein stability and local rigidity [59]. Wallon et al. [56] suggested that the substitution of a proline is defined as a flexibility substitution. This type of substitution is observed at positions 15, 121, 345 and 378 in AmyPI12, where the proline residues conserved throughout the rest of the thermophilic α-amylases are replaced by the small and hydrophobic amino acids alanine, aspartate, glutamate and aspartate in AmyPI12, respectively (Table 3). Three of these flexibility substitutions (Ala15, Asp121 and Glu378) are located in the loop regions at the surface of the molecule. The substitution of proline residues in the loop regions of AmyPI12 likely have a stabilising effect, which may allow a higher flexibility, thus enabling the enzyme to catalyze reactions at lower temperatures [54]. The side chain of the proline residues is covalently bound to the N atom of the peptide backbone, thereby restricting the rotation about N–Ca bonds and reducing the conformational flexibility of loop structures [60]. Proline avoidance in loops and turns connecting secondary structures has been noted in almost all investigated psychrophilic enzymes [61].

Many cold-adapted enzymes possess lower arginine content with respect to their mesophilic and thermophilic homologues [62, 63]. Arginine residues play a significant role in thermal adaptation and the charge resonance of the guanidinium group provides arginine the ability to form more than one salt bridge. In addition, the arginine side chain can form up to five H-bonds, preferably to carbonyl oxygens. Both structural properties of arginine certainly account for its low occurrence in psychrophilic enzymes [61]. Substitutions of arginine, which are classified as flexibility substitutions, to glutamate, alanine, asparagine and valine occurred at positions 23, 172, 214 and 481, respectively, in AmyPI12

(Table 3). Interestingly, two of these arginine substitutions (Ala172 and Val481) involved hydrophobic residues at the surface of the AmyPI12 model. It has been reported that increased structural flexibility in psychrophilic enzymes is achieved through a combination of structural features including an increase in the number of hydrophobic side chains that are exposed to the solvent. These hydrophobic surface residues destabilize protein structure due to the decreased entropy of the water molecules. The surfaces of cold-adapted enzymes have a tendency to contain a higher proportion of hydrophobic (nonpolar) residues [3, 54]. This tendency has been demonstrated by the X-ray structures of adenylate kinases from the psychrophile *Bacillus globisporus* [64].

For optimal enzyme catalysis at low temperatures, a proper balance between structural rigidity and flexibility is important to allow the retention of a specific 3D conformation at the physiological temperature and to enable the protein to perform its catalytic function. Stability substitutions were observed at amino acids 4, 56, 106, 130, 254, 301, 302 and 431 of AmyPI12 where glycines, which are conserved according to the alignment thermophilic α-amylases, are replaced by the other hydrophobic residues alanine, glutamate, aspartate and proline (Table 3). The amino acid substitution of glycine in thermophilic α-amylases with arginine in AmyPI12 occurred at position 475, which also suggests these substitutions are involved in the improved stability of the cold-adapted enzyme in the appropriate region. In addition to glycine replacement, there are other substitutions of AmyPI12 amino acids that confer protein stability to appropriate regions. These substitutions involve proline residues at locations 44, 439, 471, 472 and 474 that are replaced by other residues (alanine, glycine and asparagine) in equivalent positions of thermophilic α-amylases. All of these suggested stability substitutions in AmyPI12 support the hypothesis that psychrophilic enzymes are characterized by an improved flexibility of the structural components involved in the catalytic cycle, whereas other protein regions, if not implicated in catalysis, may be as or more rigid than their mesophilic counterparts [54, 65]. Previously, several studies have focused on whether cold-adapted proteins have flexibility throughout their structure (global flexibility) or whether they have distinct regions of local flexibility [66]. Although global flexibility has been shown to promote high activity and low stability in cold-adapted enzymes, it may also increase the possibility of incorrect folding [54]. Thus, to attain sufficient activity at low temperatures, the important domain of cold-adapted enzymes may need to be more flexible than peripheral parts of the enzyme.

Conclusions

In conclusion, this is, to our knowledge, the first report on the isolation and structural studies of an α-amylase from the psychrophilic yeast *G. antarctica* PI12. The development and analysis of a 3D model for the α-amylase AmyPI12 identified several novel characteristics of the newly isolated cold-adapted protein from *G. antarctica* PI12. The AmyPI12 model developed could be used for further comparative structural analyses to correlate the structure–activity relationships and may contribute to a better understanding of the structures and functions of other cold-adapted proteins in nature. Additional studies focused in this direction are now in progress.

Acknowledgments Special thanks to thank my colleagues Nazihah Abdul Hamid from the Universiti Teknologi Malaysia and Fathin Nur Syafiqah Jafri from the Universiti Putra Malaysia for their help and valuable discussions. This work was supported by a research grant from the Molecular Biology and Genomic Initiative Program of the Malaysia Genome Institute (Project No. 10-05-16-MB002 and 07-05-MGI-GMB014). We would also like to express our appreciation to the Malaysia Antarctic Research Programme for their support. Aizi Nor Mazila Ramli is a researcher of Universiti Teknologi Malaysia under the Post-Doctoral Fellowship Scheme.

References

1. Gianese G, Bossa F, Pascarella S (2002) Comparative structural analysis of psychrophilic and meso- and thermophilic enzymes. Proteins Struct Funct Bioinform 47:236–249
2. Zecchinon L, Claverie P, Collins T, D'Amico S, Delille D, Feller G et al (2001) Did psychrophilic enzymes really win the challenge? Extremophiles 5:313–321
3. Ramli A, Mahadi N, Shamsir M, Rabu A, Joyce-Tan K, Murad A et al (2012) Structural prediction of a novel chitinase from the psychrophilic *Glaciozyma antarctica* PI12 and an analysis of its structural properties and function. J Comput Aided Mol Des 26:947–961
4. Lu M, Wang S, Fang Y, Li H, Liu S, Liu H (2010) Cloning, expression, purification, and characterization of cold-adapted α-amylase from *Pseudoalteromonas arctica* GS230. Protein J 29:591–597
5. Machius M, Declerck N, Huber R, Wiegand G (1998) Activation of *Bacillus licheniformis* α-amylase through a disorder → order transition of the substrate-binding site mediated by a calcium sodium calcium metal triad. Structure 6:281–292
6. van der Maarel MJEC, van der Veen B, Uitdehaag JCM, Leemhuis H, Dijkhuizen L (2002) Properties and applications of starch-converting enzymes of the α-amylase family. J Biotechnol 94:137–155
7. Kuddus M, Roohi, Arif MJ, Ramteke WP (2012) Structural adaptation and biocatalytic prospective of microbial cold-active α-amylase. Afr J Microbiol Res 6:206–213
8. D'Amico S, Gerday C, Feller G (2003) Temperature adaptation of proteins: engineering mesophilic-like activity and stability in a cold-adapted α-amylase. J Mol Biol 332:981–988
9. Aghajari N, Feller G, Gerday C, Haser R (1998) Structures of the psychrophilic *Alteromonas haloplanctis* α-amylase give insights into cold adaptation at a molecular level. Structure 6:1503–1516
10. Zhang J-W, Zeng R-Y (2008) Purification and characterization of a cold-adapted α-amylase produced by *Nocardiopsis* sp. 7326 isolated from Prydz Bay, Antarctic. Mar Biotechnol 10:75–82
11. Tapia-Tussell R, Lappe P, Ulloa M, Quijano-Ramayo A, Cáceres-Farfán M, Larqué-Saavedra A et al (2006) A rapid and simple

method for DNA extraction from yeasts and fungi isolated from *Agave fourcroydes*. Mol Biotechnol 33:67–70
12. Sokolovsky VY, Kaldenhoff R, Ricci M, Russo VEA (1990) Fast and reliable mini-prep RNA extraction from *Neurospora crassa*. Fungal Genet Newslett 37:39–40
13. Stanke M, Morgenstern B (2005) AUGUSTUS: a web server for gene prediction in eukaryotes that allows user-defined constraints. Nucleic Acids Res 33:W465–W467
14. Altschul SF, Gish W, Miller W, Myers EW, Lipman DJ (1990) Basic local alignment search tool. J Mol Biol 215:403–410
15. Altschul SF, Madden TL, Schaffer AA, Zhang J, Zhang Z, Miller W et al (1997) Gapped BLAST and PSI-BLAST: a new generation of protein database search programs. Nucleic Acids Res 25:3389–3402
16. Gasteiger E, Hoogland C, Gattiker A, Duvaud SE, Wilkins MR, Appel RD et al (2005) Protein identification and analysis tools on the ExPASy server. In: John MW (ed) The proteomics protocols handbook. Humana, Totowa, pp 571–607
17. Bendtsen JD, Nielsen H, Heijne GV, Brunak S (2004) Improved prediction of signal peptides: SignalP 3.0. J Mol Biol 340:783–795
18. Gough J, Karplus K, Hughey R, Chothia C (2001) Assignment of homology to genome sequences using a library of hidden Markov models that represent all proteins of known structure. J Mol Biol 313:903–919
19. Larkin MA, Blackshields G, Brown NP, Chenna R, McGettigan PA, McWilliam H et al (2007) Clustal W and Clustal X version 2.0. Bioinformatics 23:2947–2948
20. Thompson JD, Gibson TJ, Higgins DG (2002) Multiple sequence alignment using ClustalW and ClustalX. In: Current protocols in bioinformatics. Wiley, New York
21. Kelley LA, Sternberg MJE (2009) Protein structure prediction on the Web: a case study using the Phyre server. Nat Protoc 4:363–371
22. Söding J, Biegert A, Lupas AN (2005) The HHpred interactive server for protein homology detection and structure prediction. Nucleic Acids Res 33:W244–W248
23. Fornes O, Aragues R, Espadaler J, Marti-Renom MA, Sali A, Oliva B (2009) ModLink+: improving fold recognition by using protein-protein interactions. Bioinformatics 25:1506–1512
24. Eswar N, Webb B, Marti-Renom M, Madhusudhan MS, Eramian D, Shen M-Y et al (2007) Comparative protein structure modeling using MODELLER. Curr Protoc Protein Sci 2:1–30
25. Guex N, Peitsch M (1997) SWISS-MODEL and the Swiss-Pdb Viewer: an environment for comparative protein modeling. Electrophoresis 18:2714–2723
26. Laskowski RA, Rullmann JAC, MacArthur MW, Kaptein R, Thornton JM (1996) AQUA and PROCHECK-NMR: programs for checking the quality of protein structures solved by NMR. J Biomol NMR 8:477–486
27. Colovos C, Yeates TO (1993) Verification of protein structures: patterns of nonbonded atomic interactions. Protein Sci 2:1511–1519
28. Tomii K, Hirokawa T, Motono C (2005) Protein structure prediction using a variety of profile libraries and 3D verification. Proteins Structure Function Bioinform 61:114–121
29. Bowie JU, Luthy R, Eisenberg D (1991) A method to identify protein sequences that fold into a known three-dimensional structure. Science 253:164–170
30. Luthy R, Bowie JU, Eisenberg D (1992) Assessment of protein models with three-dimensional profiles. Nature 356:83–85
31. Hunter S, Apweiler R, Attwood TK, Bairoch A, Bateman A, Binns D et al (2009) InterPro: the integrative protein signature database. Nucleic Acids Res 37:D211–D215
32. Marchler-Bauer A, Anderson JB, Derbyshire MK, DeWeese-Scott C, Gonzales NR, Gwadz M et al (2007) CDD: a conserved domain database for interactive domain family analysis. Nucleic Acids Res 35:D237–D240
33. Gan Z, Yang J, Tao N, Liang L, Mi Q, Li J et al (2007) Cloning of the gene *Lecanicillium psalliotae* chitinase *Lpchi1* and identification of its potential role in the biocontrol of root-knot nematode *Meloidogyne incognita*. Appl Microbiol Biotechnol 76:1309–1317
34. Kawase T, Saito A, Sato T, Kanai R, Fujii T, Nikaidou N et al (2004) Distribution and phylogenetic analysis of family 19 chitinases in *Actinobacteria*. Appl Environ Microbiol 70:1135–1144
35. Orikoshi H, Baba N, Nakayama S, Kashu H, Miyamoto K, Yasuda M et al (2003) Molecular analysis of the gene encoding a novel cold-adapted chitinase (ChiB) from a marine bacterium, *Alteromonas* sp. Strain O-7. J Bacteriol 185:1153–1160
36. Wahab H, Ahmad Khairudin N, Samian M, Najimudin N (2006) Sequence analysis and structure prediction of type II *Pseudomonas* sp. USM 4–55 PHA synthase and an insight into its catalytic mechanism. BMC Struct Biol 6:23
37. Ramachandran GN, Ramakrishnan C, Sasisekharan V (1963) Stereochemistry of polypeptide chain configurations. J Mol Biol 7:95–99
38. Matsuura Y, Kusunoki M, Harada W, Tanaka N, Iga Y, Yasuoka N et al (1980) Molecular structure of Taka-Amylase A: I. Backbone chain folding at 3 A resolution. J Biochem 87:1555–1558
39. Robert X, Haser R, Mori H, Svensson B, Aghajari N (2005) Oligosaccharide binding to barley α-amylase 1. J Biol Chem 280:32968–32978
40. Declerck N, Machius M, Wiegand G, Huber R, Gaillardin C (2000) Probing structural determinants specifying high thermostability in *Bacillus licheniformis* α-amylase. J Mol Biol 301:1041–1057
41. Ben Abdelmalek I, Urdaci MC, Ben Ali M, Denayrolles M, Chaignepain S, Limam F et al (2009) Structural investigation and homology modeling studies of native and truncated forms of α-amylases from *Sclerotinia sclerotiorum*. J Microbiol Biotechnol 19:1306–1318
42. Kanai R, Haga K, Akiba T, Yamane K, Harata K (2004) Biochemical and crystallographic analyses of maltohexaose-producing amylase from alkalophilic *Bacillus* sp. 707. Biochemistry 43:14047–14056
43. Oudjeriouat N, Moreau Y, Santimone M, Svensson B, Marchis-Mouren G, Desseaux V (2003) On the mechanism of α-amylase. Eur J Biochem 270:3871–3879
44. Watanabe K, Miyake K, Suzuki Y (2001) Identification of catalytic and substrate-binding site residues in *Bacillus cereus* ATCC7064 oligo-1,6-glucosidase. Biosci Biotechnol Biochem 65:2058–2064
45. Suvd D, Fujimoto Z, Takase K, Matsumura M, Mizuno H (2001) Crystal structure of *Bacillus stearothermophilus* α-amylase: possible factors determining the thermostability. J Biochem 129:461–468
46. Feller G, Payan F, Theys F, Qian M, Haser R, Gerday C (1994) Stability and structural analysis of α-amylase from the antarctic psychrophile *Alteromonas haloplanctis* A23. Eur J Biochem 222:441–447
47. Vihinen M, Mantsala P (1990) Characterization of a thermostable *Bacillus stearothermophilus* alpha-amylase. Biotechnol Appl Biochem 12:427–435
48. Okubo Y, Yokoigawa K, Esaki N, Soda K, Kawai H (1999) Characterization of psychrophilic alanine racemase from *Bacillus psychrosaccharolyticus*. Biochem Biophys Res Commun 256:333–340
49. Schlatter D, Kriech O, Suter F, Zuber H (1987) Structure and function of L-lactate dehydrogenase from thermophilic, mesophilic and psychrophilic bacteria, VIII. The primary structure of the psychrophilic lactate dehydrogenase from *Bacillus psychrosaccharolyticus*. Biol Chem Hoppe Seyler 368:1435–1446
50. Vckovski V, Schlatter D, Zuber H (1990) Structure and function of L-lactate dehydrogenases from thermophilic, mesophilic and psychrophilic bacteria, IX. Identification, isolation and nucleotide

sequence of two L-lactate. dehydrogenase genes of the psychrophilic bacterium *Bacillus psychrosaccharolyticus*. Biol Chem Hoppe Seyler 371:103–110
51. Kagawa M, Fujimoto Z, Momma M, Takase K, Mizuno H (2003) Crystal structure of *Bacillus subtilis* α-amylase in complex with acarbose. J Bacteriol 185:6981–6984
52. Alikhajeh J, Khajeh K, Ranjbar B, Naderi-Manesh H, Lin Y-H, Liu E et al (2010) Structure of *Bacillus amyloliquefaciens* α-amylase at high resolution: implications for thermal stability. Acta Crystallogr F 66:121–129
53. Joyet P, Declerck N, Gaillardin C (1992) Hyperthermostable variants of a highly thermostable alpha-amylase. Nat Biotechnol 10:1579–1583
54. Siddiqui KS, Cavicchioli R (2006) Cold-adapted enzymes. Annu Rev Biochem 75:403–433
55. Watanabe S, Yasutake Y, Tanaka I, Takada Y (2005) Elucidation of stability determinants of cold-adapted monomeric isocitrate dehydrogenase from a psychrophilic bacterium, *Colwellia maris*, by construction of chimeric enzymes. Microbiology 151:1083–1094
56. Wallon G, Lovett S, Magyar C, Svingor A, Szilagyi A, Zavodszky P et al (1997) Sequence and homology model of 3-isopropylmalate dehydrogenase from the psychrotrophic bacterium *Vibrio* sp. I5 suggest reasons for thermal instability. Protein Eng 10:665–672
57. Galkin A, Kulakova L, Ashida H, Sawa Y, Esaki N (1999) Cold-adapted alanine dehydrogenases from two Antarctic bacterial strains: gene cloning, protein characterization, and comparison with mesophilic and thermophilic counterparts. Appl Environ Microbiol 65:4014–4020
58. Feller G, Arpigny JL, Narinx E, Gerday C (1997) Molecular adaptations of enzymes from psychrophilic organisms. Comp Biochem Physiol A Physiol 118:495–499
59. Herning T, Yutani K, Inaka K, Kuroki R, Matsushima M, Kikuchi M (1992) Role of proline residues in human lysozyme stability: a scanning calorimetric study combined with x-ray structure analysis of proline mutants. Biochemistry 31:7077–7085
60. Davail S, Feller G, Narinx E, Gerday C (1994) Cold adaptation of proteins. Purification, characterization, and sequence of the heat-labile subtilisin from the antarctic psychrophile *Bacillus* TA41. J Biol Chem 269:17448–17453
61. Feller G, Gerday C (1997) Psychrophilic enzymes: molecular basis of cold adaptation. Cell Mol Life Sci 53:830–841
62. Garsoux G, Lamotte J, Gerday C, Feller G (2004) Kinetic and structural optimization to catalysis at low temperatures in a psychrophilic cellulase from the Antarctic bacterium *Pseudoalteromonas haloplanktis*. Biochem J 384:247–253
63. Feller G (2003) Molecular adaptations to cold in psychrophilic enzymes. Cell Mol Life Sci 60:648–662
64. Bae E, Phillips GN (2004) Structures and analysis of highly homologous psychrophilic, mesophilic, and thermophilic adenylate kinases. J Biol Chem 279:28202–28208
65. Georlette D, Blaise V, Collins T, D'Amico S, Gratia E, Hoyoux A et al (2004) Some like it cold: biocatalysis at low temperatures. FEMS Microbiol Rev 28:25–42
66. Paredes D, Watters K, Pitman D, Bystroff C, Dordick J (2011) Comparative void-volume analysis of psychrophilic and mesophilic enzymes: structural bioinformatics of psychrophilic enzymes reveals sources of core flexibility. BMC Struct Biol 11:1–9